Supporting Information:

Materials

The nanodiamonds were produced according to the procedure described in [1]. The horse-spleen ferritin was obtained from Sigma-Aldrich.

Preparation of ND/ferritin complex

10 mg Ferritin and carboxylated ND (1 mg) were incubated for 2h in 10 mL boric acid buffer (5mM, pH 8.5). pH was adjusted with 0.1 M NaOH aqueous solution. The resulting ferritin-diamond mixture went through several circles of washing with deionized water until all the free ferritin was removed. The purification procedure was monitored by TEM image.

Transmission Electron Microscope (TEM)

In figure S1 a TEM image of the ND/ferritin complex is shown, before it is purified from the residual free ferritin. Single ferritin and NDs can be observed.

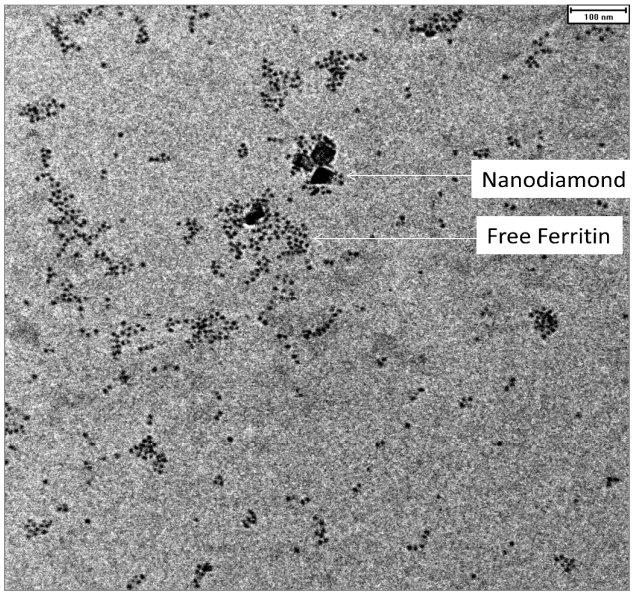

Figure S1a TEM image of unpurified ND/ferritin complex.

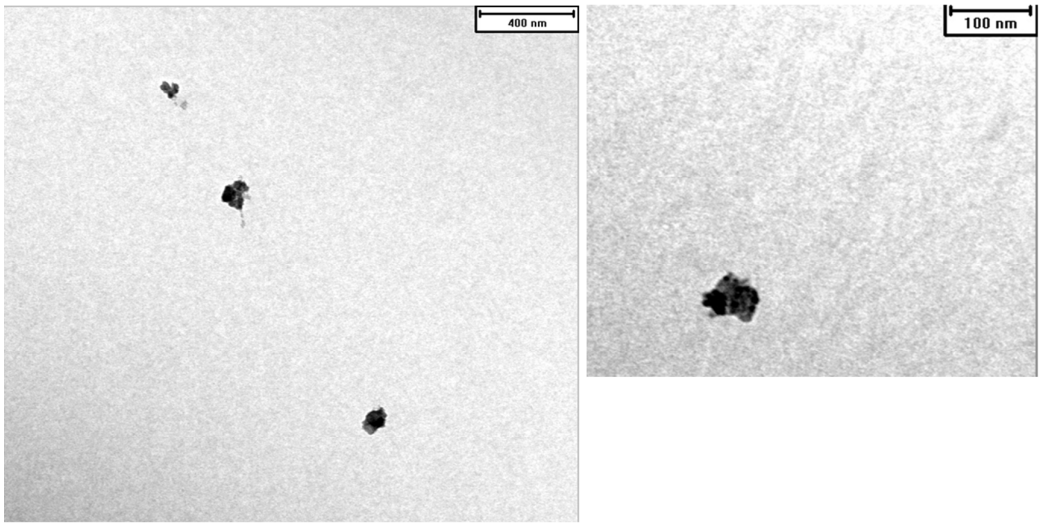

Figure S1b TEM image of ND/ferritin complex purified by centrifugation.

Fourier transform infrared spectroscopy (FTIR) measurements

Figure S2a shows the FTIR spectrum of nanodiamonds. Several distinct features appear at 3435 cm^{-1} and 1634 cm^{-1}. These two peaks can be assigned to the O-H stretch of the surface carboxyl group and to the C=O stretching of the carboxylate anion. The associated hydrogen bonds between physically adsorbed water molecules are responsible for the broad absorption bands observed at 3000-3600 cm^{-1}. FTIR spectrum of the ND/ferritin complex is depicted in Figure S2b. The lines approximately at 1654 $cm^{-1}$and 1534 cm^{-1} correspond to the amide I and amide II bands, respectively, which are specific for a peptide bond in proteins. A broad absorption envelope in the low frequency region (700–400 cm^{-1}) was observed in nanodiamond-ferritin spectra. The ferrihydrite peak appears at 576 cm^{-1}

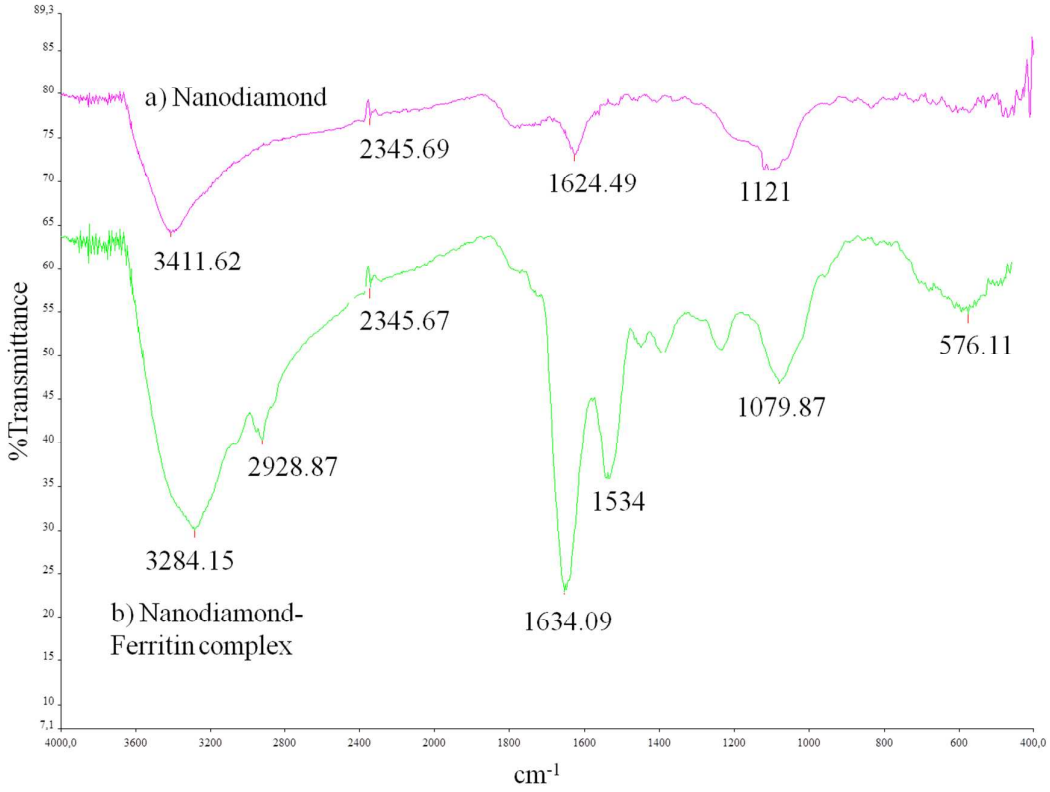

Figure S2: FTIR spectroscopy of nanodiamond (a) and ND/ferritin complex (b).

Dynamic Light Scattering (DLS) measurements

Dynamic light scattering (DLS) has been used to characterize the nanodiamond-ferritin complex in solution. The hydrodynamic diameter of the resultant nanoparticles has been measured using a commercial system {Nano Zetasizer (Malvern Instruments)}. All the DLS experiments have been performed with a laser wavelength of 633 nm at 25±0.1 ^{0}C and a fixed backscattering angle of 173^{0}C. The mean hydrodynamic diameter was determined by cumulative analysis. The sample was filtered in advance by a 0.2 μm microsyringe filter to avoid any dust contaminations.

DLS measurements reveal that "free" NDs have an average hydrodynamic diameter 30.1±0.2 nm (Figure S3a). After adsorption of ferritin the diameter of was determined to be 84.5 ± 3.8 nm (Figure S3b). The large increase could be explained by the presence of the iron ions on the diamond surface, leading to higher concentration of surface charges, thus attracting more water molecules. This effect is an indirect confirmation that the ferritin is attached to the diamond surface.

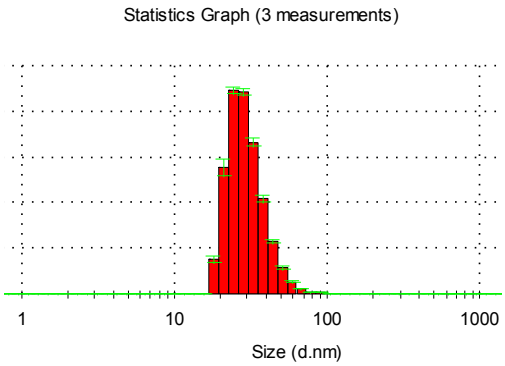

Figure S3a. Number size distributions of nanodiamonds determined by DLS. The average hydrodynamic diameter is 30.1 ± 0.2 nm. The results were obtained after three independent measurements.

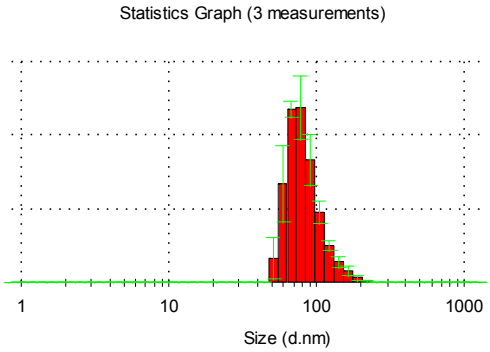

Figure S3b. Number size distributions of ND/ferritin complex. The average hydrodynamic diameter is 83.8 ± 2.7 nm. The results were obtained after three independent measurements.

Zeta Potential measurements

Measurements of the zeta-potential in solution at pH = 7 of "free" NDs reveal negative values of -40.9±0.7 mV, probably due to the presence of several deprotonated carboxylic acid groups. "Free" ferritin molecules show much higher, but still negative value of -20.13 mV. The zeta-potential of the joint complex decreases further down to -46.9 ± 1.1 mV, possibly due to the formation of additional negative surface charges, thus increasing the electrophoretic velocity of the ND–Ferritin complex.

X-ray photoelectron spectroscopy (XPS) study

X-ray photoelectron spectroscopy (XPS) has been additionally used to obtain information about the elemental composition of ND-Ferritin complex. The spectrum of ND/ferritin complex shown in Figure S4 reveals the presence of iron. The 2p transition of the latter is observed at 711eV and 3s and 3p transitions exhibit binding energy peaks at 95 eV and 53 eV respectively.

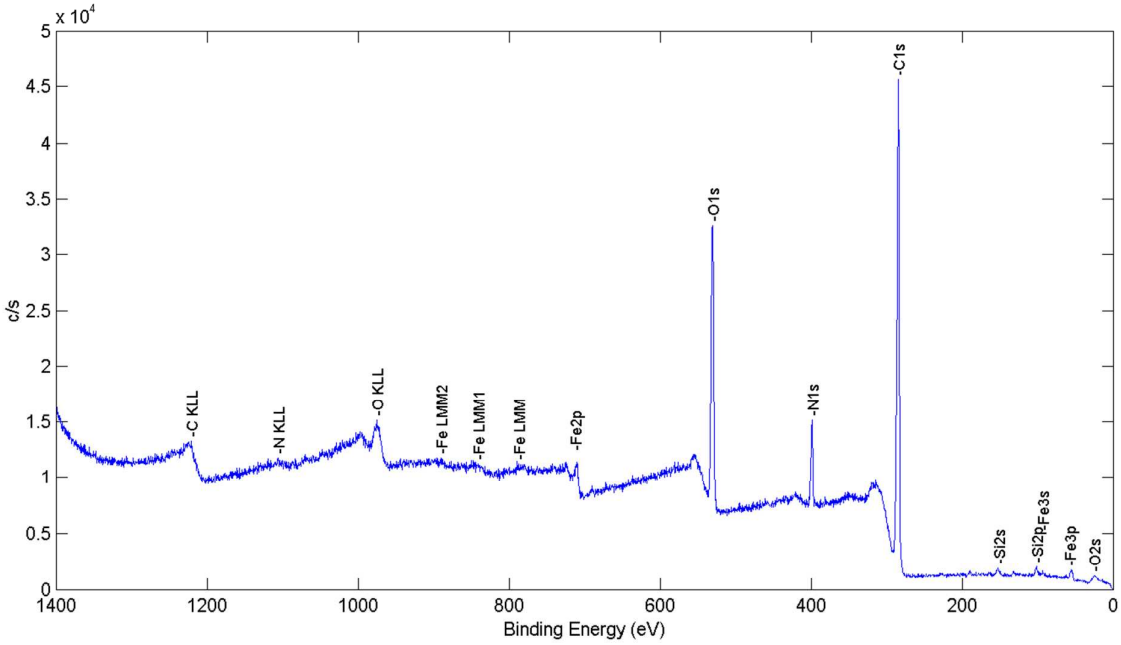

Figure S4. XPS spectrum of ND/ferritin complex, showing the presence of iron.

Numerical simulation of the fluctuating field from ferritin

In order to numerically estimate the effect of the ferritin molecules on the decoherence times of NV centers, we include around 4500 iron Fe(III) (electron spin S = 5/2) using the geometry of a ferrihydrite mineral $[FeO(OH)]_8[FeO(H_2PO_4)]$ [2]. Each iron provides magnetic field acting on NV centers depending on its spins state m_S and its position $\vec{r} = r \cdot (\hat{r}_x, \hat{r}_y, \hat{r}_z)$, which can be written as $\vec{b}(\vec{r}) = (b_x, b_y, b_z)$ with the transverse components $b_x(\vec{r}) = \frac{\mu_0}{4\pi}\frac{\gamma^2}{r^3}(3\hat{r}_x\hat{r}_z)m_s$, $b_y(\vec{r}) = \frac{\mu_0}{4\pi}\frac{\gamma^2}{r^3}(3\hat{r}_y\hat{r}_z)m_s$ and the longitudinal component $b_z(\vec{r}) = \frac{\mu_0}{4\pi}\frac{\gamma^2}{r^3}(3\hat{r}_z\hat{r}_z - 1)m_s$. We model the fluctuation of such a magnetic field as a classical process, namely the iron spins exchange polarization randomly at a certain rate g, which is determined to match the spectral width of the ESR signal of ferritin measured in obtained in independent experiments and takes the value g = 2.1 GHz [3]. We start from about 1000 initial iron spin configurations and simulate the total fluctuating magnetic fields coming from all the irons and acting on the NV centers. Considering the structure of the ND/ferritin complex determined in our experiment, we include 8-15 ferritins with random orientations to NV, where the ferritins are arranged in such a way that the distance from each ferritin to NV centers is above 12 nm, and the center-to-center distances between Ferritins is randomly distributed in the range of [9nm, 35nm] to be consistent with the size of ferritin itself and the size of the nanodiamonds.

The transversal component of the fluctuating magnetic field $b_x(t)$, $b_y(t)$ from the Fe(III) spins leads to the relaxation of the NV center and shortens the value of T_1. The Fourier transform of this field provides us with the noise spectrum $S^{\perp}(\omega)$, see Figure S5 for an example of this noise spectrum from a ferritin with a distance of 20 nm from NV center. The noise spectrum at the frequency corresponding to the NV centers' zero field splitting (i.e. ω_0=2.87 GHz) gives the estimation of T_1 as $1/S^{\perp}(\omega=\omega_0)$. The the NV centers' zero field splitting is therefore $\omega_0 \approx 1.36g$. In the following, we use the same parameter to estimate the distribution of T_2, and compare with the experimental data.

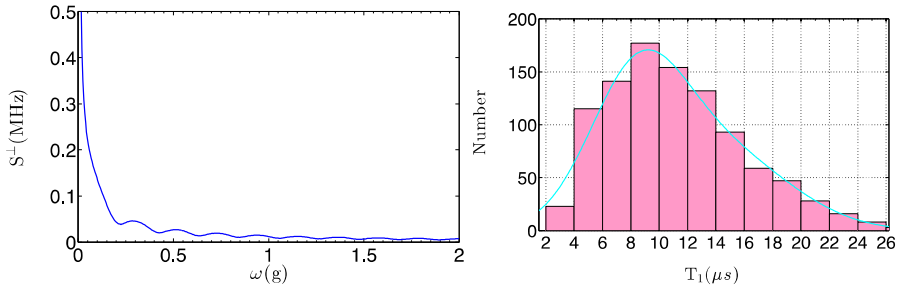

Figure S5 Left: The transversal field noise spectrum from a ferritin at a distance of 20 nm from a NV center. We have averaged over different ferritin-NV orientations. The rate is chosen as the frequency unit in the plot. Right: The distribution of T_1 from numerical simulation from around 10^3 with randomly 8-15 distributed Ferritins.

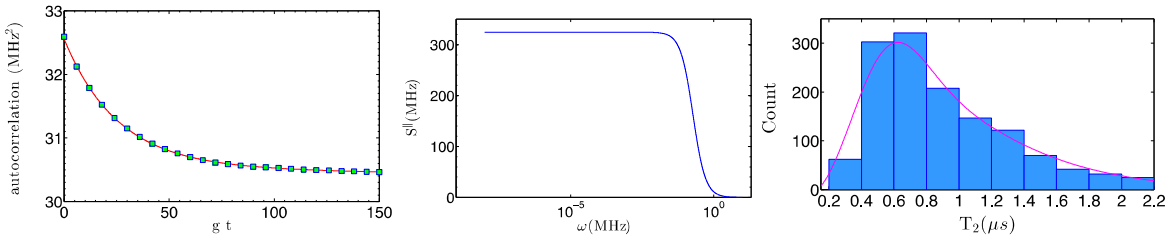

Figure S6 Left: The auto-correlation function of the longitudinal field from a ferritin at a distance of 20 nm from a NV center. We have averaged over different ferritin-NV orientations. Middle: The corresponding longitudinal noise spectrum using the same parameter g = 2.1 GHz as in our estimation for T_1. Right: The distribution of T_1 from numerical simulation from around 10^3 with randomly 8-15 distributed ferritin molecules.

To estimate T_2, we calculate the auto-correlation function of the longitudinal component of the fluctuating field $b_z(t)$ from Ferritins, which is defined as $S^{//}(t)=\langle b_z(t_0)b_z(t_0+t)\rangle$. The Fourier transformation of $S^{//}(t)$ gives us the longitudinal noise spectrum $S^{//}(\omega)$. In Figure S6, we plot $S^{//}(t)$ and the corresponding noise spectrum. The decay of the spin echo signal SE can be calculated [4] as $SE(t)=8\int_0^{\infty}\frac{d\omega}{\pi}S^{//}(\omega)\sin^4\left(\frac{\omega t}{4}\right)\frac{1}{\omega^2}$. By calculating the decay of the spin echo signal, we can estimate the value of T_2, which is given by $SE(t=T_2)=\exp(-1)$, see also Figure S6.

References:

[1] Y. Chang, H. Lee, K. Chen, C.Chang, D.Tsai, C. Fu, T. Lim, Y. Tzeng, C.Fang, C. Han, H.C. Chang and W. Fann, *Nat. Nanotechnol.,* 2008. **3**, 284

[2] K. L.Taft , G. C. Papaefthymiou, S. J. Lippard, A Mixed-Valent Polyiron Oxo Complex That Models the Biomineralization of the Ferritin Core, Science, 1993, **259**, 1302.

[3] E. Wajnberg, L. J. El-Jaick, M. P. Linhares, and D. M. S. Esquivel, Ferromagnetic Resonance of Horse Spleen Ferritin: Core Blocking and Surface Ordering Temperatures, Journal of Magnetic Resonance, 2001, **153,** 69.

[4] L. Cywiński, R. M. Lutchyn, C. P. Nave, and S. Das Sarma, How to enhance dephasing time in superconducting qubits, Phys. Rev. B 77, 174509 (2008).